KWANG-PIL JEONG*, JEONG-GON KIM*#, SU-WON YANG*,
JAE-HO YUN*, JIN-HYUK CHOI*

STUDY ON MAGNETIC PROPERTIES OF THE U-TYPE FERRITE ACCORDING TO SUBSTITUTED ELEMENTS

The magnetic properties of the U-type ferrite synthesized by a sol-gel process had studied by substituting cobalt with manganese or zinc in cobalt-based U-type ferrite. The substituted U-type ferrite showed a dominant crystal structure at a different substitution ratio of manganese and zinc. The change of the starting temperature of U-type ferrite formation according to substitutional elements was confirmed by TG-DTA analysis. In the case of manganese substitution, the starting temperature of U-type ferrite formation lowered, and on the contrary, when zinc was substituted, it became higher. The magnetic properties of the U-type ferrite substituted with manganese showed a tendency that the saturation magnetization was decreased and the coercivity was increased as the manganese ratio increased. The highest saturation magnetization was 57.9 emu/g in the specific composition ($Ba_4Co_{0.5}Zn_{1.5}Fe_{36}O_{60}$) substituted with zinc.

Keywords: U-type ferrite, hexagonal ferrite, sol-gel process

1. Introduction

The U-type ferrite is represented by the general formula $A_4B_2Fe_{36}O_{60}$ where A is a heavy alkaline earth metal and B is a divalent transition metal. It belongs to the hexagonal ferrite. The hexagonal ferrite has various stable phases such as M, Y, W, Z, X, and U-type [1,2]. Among them, the U-type ferrite has the most complex crystal structure and a large unit cell [3]. The hexagonal ferrite has been mainly used as a microwave absorber in the GHz frequency range due to the high saturation magnetization and the large intrinsic magnetocrystalline anisotropy [4,5]. The conventional U-type ferrite studies have been fabricated by a ceramic process (or solid state reaction process) [6-14].

The unit cell of U-type ferrite is represented by 2M+Y where M is $AO \cdot 6Fe_2O_3$ and Y is $2AO \cdot 2BO \cdot 6Fe_2O_3$ (A: barium, strontium, B: manganese, iron, cobalt, nickel, zinc, etc.). In this crystal structure, the oxygen anion (O^{2-}) and heavy alkaline earth metal cations (A^{2+}) are closed-packed to form a lattice, and the cations (Fe^{3+} or B^{2+}) are located at the octahedral, tetrahedral, and trigonal sites. The radius of the oxygen anion and heavy alkaline earth metal cations is 118-140 pm and the radius of the transition metal cations is 60-74 pm [6]. Its small cations determine the magnetic properties of the materials.

Therefore, in this study, we investigated the change in magnetic property depending on the kind and composition of cations. The reference U-type ferrite was synthesized with $Ba_4Co_2Fe_{36}O_{60}$ (Co₂U) containing barium in the A site and cobalt in the B site. This composition is based on our previous studies using the sol-gel process. The saturation magnetization of the reference U-type ferrite has ~51 emu/g, that is similar to the conventional ceramic process [7,15]. We aim to investigate the effect of substituting the Co^{2+} ion sites with different divalent transition metal ions.

2. Experimental

In this study, the U-type ferrites were synthesized by the sol-gel process. The starting materials were barium nitrate ($Ba(NO_3)_2$, 98.5%), cobalt acetate tetrahydrate ($Co(CH_3COO)_2 \cdot 4H_2O$, 98.0%), zinc acetate dihydrate ($Zn(O_2C_2H_3)_2 \cdot 2H_2O$, 97.0%), manganese nitrate tetrahydrate ($MnN_2O_6 \cdot 4H_2O$, 98.0%), iron nitrate nonahydrate ($Fe(NO_3)_3 \cdot 9H_2O$, 98.5%), which were mixed in deionized water at the designed stoichiometry ratio. Citric acid ($C_6H_8O_7$, 99.0%), ethylene glycol ($C_2H_6O_2$, 98.5%) were added to the mixture and adjusted to the pH 6 by ammonia solution. An additional reflux system for keeping the concentration of the mixture was applied in a sol reaction. After the reaction was completed, a sol was stirred and heated to 85°C for 8 hours. Then it was heat treated at 1200-1300°C for 3 hours in the atmosphere.

The identification of the U-type ferrite was analyzed by XRD (Rigaku, Cu K_α, $\lambda = 0.154$ nm, $2\theta = 20$-80°). The thermal behavior of synthesized the U-type ferrite was confirmed by TG-

*   INCHEON NATIONAL UNIVERSITY, DEPARTMENT OF MATERIALS SCIENCE AND ENGINEERING, 119 ACADEMY-RO, YEONSU-GU, INCHEON, 22012, KOREA

\#   Corresponding author: jyj309@inu.ac.kr

DTA (PerkinElmer, STA8000). The morphology and size of the U-type ferrite were observed by FE-SEM (JEOL, JSM-7800F). The magnetic properties according to the substituted element was measured using a VSM (Quantum Design, VersaLab VSM, ±10,000 Oe, room temperature).

3. Results and discussion

In our latest study, it was confirmed that the cobalt based on the U-type ferrite (Co_2U) formation was depended on a heat treatment temperature. The heat treatment condition for the formation of the U-type ferrite was 1300°C for 3 hours [15]. In order to investigate the effect of substituted elements and their ratios on the U-type formation temperature, XRD patterns were confirmed at 1200-1300°C (Fig. 1). As can be seen from the XRD pattern, it was in agreement with the XRD pattern of the U-type ferrite synthesized by the conventional solid-state reaction process [10]. In Fig. 1(b) and (d), which heat-treated samples at 1300°C, the XRD patterns of $Ba_4Co_{0.5}Mn_{1.5}Fe_{36}O_{60}$ ($x = 1.5$), $Ba_4Mn_2Fe_{36}O_{60}$ ($x = 2.0$), $Ba_4Co_{1.5}Mn_{0.5}Fe_{36}O_{60}$ ($y = 0.5$) and

$Ba_4CoMnFe_{36}O_{60}$ ($y = 1.0$) were similar to 1200°C's. It was indicated that the intermediate phase was formed or the U-type ferrite begins to be formed at 1300°C in some of the substitutional compositions.

Fig. 2 shows the TG-DTA curve for the samples, which the U-type ferrite was dominantly formed. Samples were prepared as a powder in which the gel was dried at 120°C for 24 hours. The TG-DTA analysis proceeded 30 to 1300°C at a heating rate of 5°C/min. Fig. 2(a) was represented $Ba_4Co_2Fe_{36}O_{60}$ (Co_2U), (b) $Ba_4CoMnFe_{36}O_{60}$ (CoMnU) with 1:1 ratio of cobalt and manganese, and (c) $Ba_4Co_{0.5}Zn_{1.5}Fe_{36}O_{60}$ ($Co_{0.5}Zn_{1.5}U$) with cobalt 1.5 substituted with zinc. Fig. 2(a) was observed the mass loss of 52 wt% at 30-250°C and the mass loss of 20 wt% at 250-370°C, respectively. The mass loss in this region was due to the removal of water from the sample, which was confirmed by the endothermic peak of the DTA curve. In the region above 370°C, a broad exothermic region was maintained with a slight mass loss and an exothermic peak was observed at 1211°C. A broad exothermic region above 370°C was indicated that the Co_2U was formed continuously from M-type and Y-type ferrite. It is the reason why it is difficult to obtain a single phase of the U-
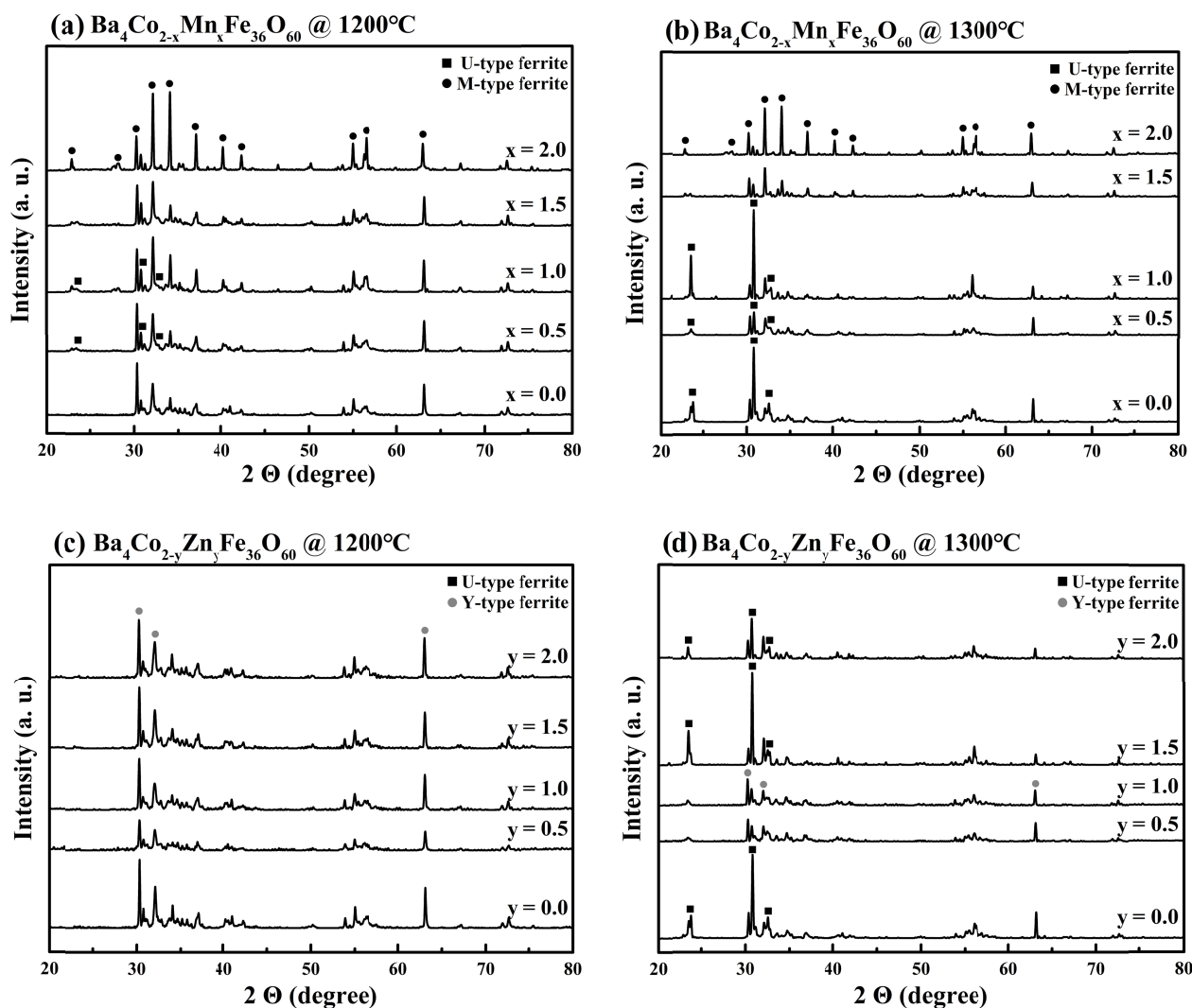

Fig. 1. XRD pattern of U-type ferrite with substitution ratio and heat-treated temperature; $Ba_4Co_{2-x}Mn_xFe_{36}O_{60}$ series at (a) 1200°C and (b) 1300°C, $Ba_4Co_{2-y}Zn_yFe_{36}O_{60}$ series at (c) 1200°C, and (d) 1300°C

(a) Ba₄Co₂Fe₃₆O₆₀

(b) Ba₄CoMnFe₃₆O₆₀

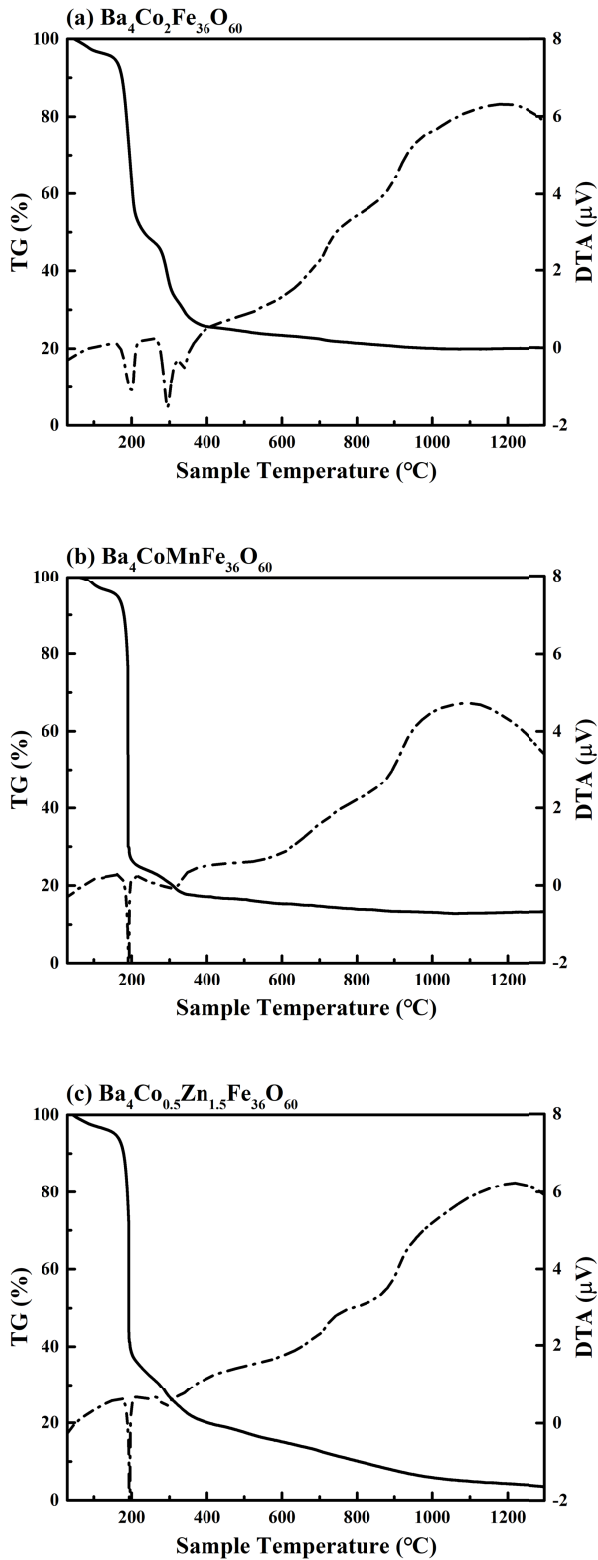**(c) Ba₄Co₀.₅Zn₁.₅Fe₃₆O₆₀**

Fig. 2. TG-DTA curve of the U-type ferrite for the heating to 1300°C with a heating rate of 5°C/min; (a) Co_2U, (b) CoMnU and (c) $Co_{0.5}Zn_{1.5}U$

type ferrite with the complex crystal structure. The TG curve of Fig. 2(b) was observed the mass loss of 75 wt% at 30-220°C and the mass loss of 8 wt% at 220-245°C. This region was also the water evaporation period as Co_2U sample (Fig. 2(a)). And a broad exothermic region was observed in the region above 345°C, but the exothermic peak was shifted to a low temperature of 1105°C.

As shown in Fig. 1(a), even a small fraction of the U-type ferrite was observed at 1200°C XRD pattern. This suggests that the DTA analysis can indirectly confirm the starting temperature of the U-type ferrite formation. However, the exothermic peak of the DTA curve indicates the starting temperature of the U-type ferrite formation, which does not mean that the U-type ferrite is formed throughout the sample. As can be seen from the XRD pattern, the dominant form of U-type ferrite required a heat treatment at 1300°C. A slight difference was observed in the TG curve of Fig. 2(c). The mass loss by water removal was the same, but continuous mass loss was observed after 370°C. The mass loss during the formation of the U-type ferrite was observed in all of Fig. 2(a)-(c). The mass loss of each sample was (a) 8 wt%, (b) 7 wt%, and (c) 14 wt%. Conversion to weight loss resulted in (a) 0.4 mg, (b) 0.4 mg, and (c) 0.5 mg, respectively. It is a slight difference. And it was confirmed that the exothermic peak was shifted to a high temperature of 1221°C. The XRD pattern in Fig. 1 (c) shows that the formation of the U-type ferrite did not start at 1200°C.

Fig. 3 shows SEM images of the dominant and non-dominant samples of the U-type ferrite. Fig. 3(a), (b) and (c) are represented Co_2U, CoMnU, and $Co_{0.5}Zn_{1.5}U$ heat-treated samples at 1300°C for 3hours, respectively. It was observed plate-shaped grains were connected. Fig. 3(d), (e) and (f) show a difference from Fig. 3(a)-(c). Fig. 3(d) shows the case where only a small fraction of the U-type ferrite was formed from the Co_2U sample heat-treated at 1200°C. As compared with Fig. 3(a), the grains retained their submicron size. Fig. 3 (e) shows the Mn_2U ($Ba_4Mn_2Fe_{36}O_{60}$) sample heat-treated sample at 1300°C for 3hours. It was observed that submicron-sized grains were ag-glomerated. Fig. 3(f) shows the $Co_{0.5}Zn_{1.5}U$ heat-treated sample at 1200°C for 3 hours and similar to size and morphology that the Co_2U sample at the same temperature.

Fig. 4 and 5 show the change in magnetic properties (*M-H* curve) with the substitution ratio in the compositions dominated by the form of U-type ferrite. And Table 1 was listed the satura-tion magnetization (M_s) and the coercivity (H_c) in each sample. In the manganese substituted samples (Fig. 4), the M_s was decreased with increasing substitution ratio from 51.4 emu/g to 46.6 emu/g. The decrease in M_s was reported to be due to the conversion of Fe^{3+} ($5\mu_B$) ions of the octahedral site to Fe^{2+} ($4\mu_B$) ions as manganese was substituted [8]. In Fig. 5, the M_s of the sample in which the zinc was substituted by 1.5 was increased to 57.9 emu/g. It was due to the enhancement of the superexchange interaction with the Fe^{3+} ions of the octahedral site, oxygen ions, and the Fe^{3+} ions of the trigonal bi-pyramidal site [9]. And the M_s of the sample in which the cobalt was substituted with zinc was decreased to 48.5 emu/g. It was the effect of the substituted Zn^{2+} ions. The Co^{2+} ($3\mu_B$) and Zn^{2+} ($0\mu_B$) have different Bohr magneton. Unlike the M_s change with the substituted element and its ratio, it was found that H_c tended to increase with increasing substitution ratio in all substituted samples. The H_c was increased from 55.4 Oe of the unsubstituted sample to 128.3-131.1 Oe. The increase in the H_c was attributed to the enhancement of the magnetocrystalline anisotropy [15-17].
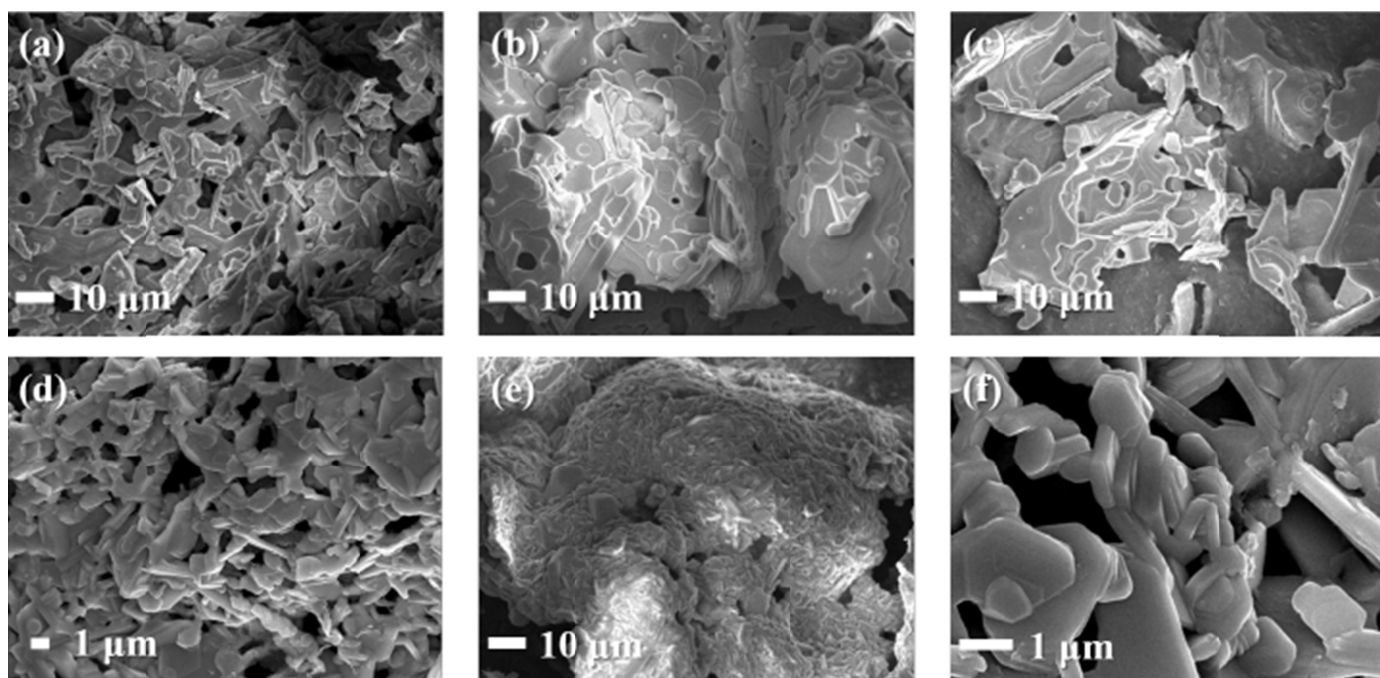
Fig. 3. SEM image of the U-type ferrite at different composition and heat-treated temperature; (a) Co_2U heat-treated at 1300°C, (b) CoMnU heat-treated at 1300°C, (c) $Co_{0.5}Zn_{1.5}U$ heat-treated at 1300°C, (d) Co_2U heat-treated at 1200°C, (e) Mn_2U heat-treated at 1300°C and (f) $Co_{0.5}Zn_{1.5}U$ heat-treated at 1200°C
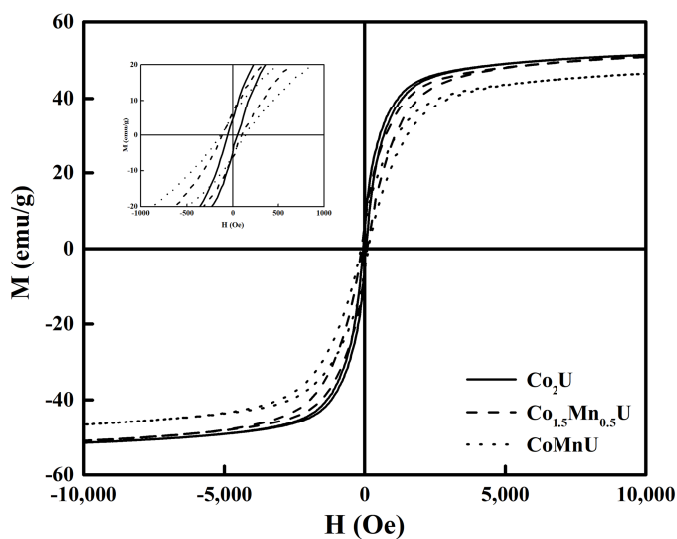

Fig. 4 The *M-H* curve according to manganese substituted ratio and the inset shows an enlarged view in the magnetic field range −1k Oe ≤ *H* ≤ 1k Oe
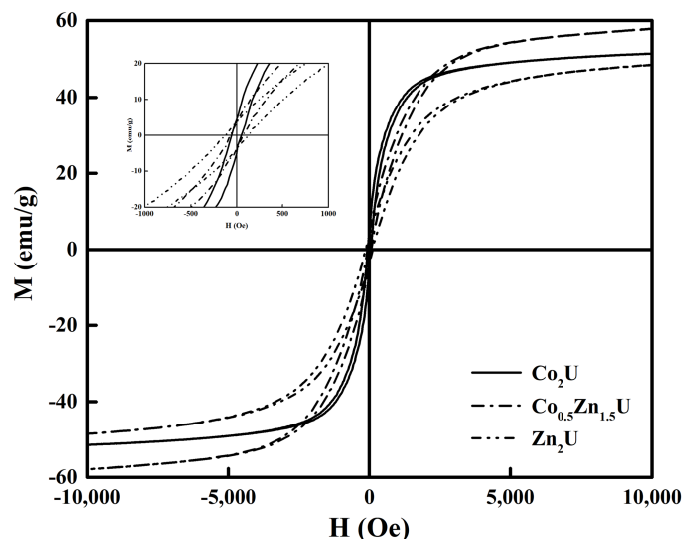
Fig. 5. The *M-H* curve according to zinc substituted ratio and the inset shows an enlarged view of in the magnetic field range −1k Oe ≤ *H* ≤ 1k Oe

4. Conclusions

The substituted U-type ferrite samples were prepared by the sol-gel process. The substitution elements were manganese and zinc, which the divalent transition metal. In XRD patterns, the U-type ferrite dominantly appeared in some of the substitution compositions. The samples with dominant U-type ferrite crystal structure were 0.5 and 1.0 substituted manganese and 1.5 and 2.0 substituted zinc. DTA analysis of the samples prepared in each composition was able to confirm the starting temperature of the U-type ferrite formation. The U-type ferrite formation

TABLE 1

Magnetic properties of the U-type ferrite according to the substituted element ratio

Sample	Composition	M_s (emu/g)	H_c (Oe)
Co_2U	$Ba_4Co_2Fe_{36}O_{60}$	51.4	55.4
$Co_{1.5}Mn_{0.5}U$	$Ba_4Co_{1.5}Mn_{0.5}Fe_{36}O_{60}$	50.9	98.8
CoMnU	$Ba_4Co_{1.0}Mn_{1.0}Fe_{36}O_{60}$	46.6	131.1
$Co_{0.5}Zn_{1.5}U$	$Ba_4Co_{0.5}Zn_{1.5}Fe_{36}O_{60}$	57.9	66.6
Zn_2U	$Ba_4Zn_2Fe_{36}O_{60}$	48.5	128.2

starting temperature of the manganese substituted 1.0 sample was lowered to 1105°C, while the zinc substituted 1.5 sample was increased to 1221°C. In the samples that U-type ferrite was dominantly formed, grains were connected to each other. The magnetic properties of the substituted samples were affected by the type and ratio of substitution elements. In the manganese substituted samples, the soft magnetic properties inherent to the U-type ferrite were maintained, while the decrease of saturation magnetization and the increase of coercivity were observed with increasing substitution ratio. In the zinc substituted samples, increasing of saturation magnetization was observed for a particular composition, and it was 57.9 emu/g in $Ba_4Co_{0.5}Zn_{1.5}Fe_{36}O_{60}$.

REFERENCES

[1]   D. Lisjaka, P. McGuiness, M. Drofenik, J. Mater. Res. **19**, 2462 (2004).

[2]   D. Lisjaka, P. McGuiness, M. Drofenik, J. Mater. Res. **21**, 420 (2006).

[3]   R.C. Pullar, Prog. Mater. Sci. **57**, 1191 (2012).

[4]   S.R. Shannigrahi, W.Q. Au, V.S. Kumar, L. Liu, Z.H. Yang, C. Cheng, C.K.I. Tan, R.V. Ramanujan, J. Magn. Magn. Mater. **325**, 63 (2013).

[5]   M.C. Dimri, H. Khanduri, H. Kooskora, I. Heinmaa, E. Joon, R. Stern, J. Magn. Magn. Mater. **323**, 2210 (2011).

[6]   K. Kamishima, R. Tajima, K. Watanabe, K. Kakizaki, A. Fujimori, M. Sakai, K. Watanabe, H. Abe, J. Magn. Magn. Mater. **375**, 54 (2015).

[7]   R.S. Meena, S. Bhattacharya, R. Chatterjee, Mater. Sci. Eng. B **171**, 133 (2010).

[8]   R.S. Meena, S. Bhattacharya, R. Chatterjee, Mater. Des. **31**, 3220 (2010).

[9]   S. Kumar, R Chatterjee, J. Magn. Magn. Mater. **448**, 88 (2018).

[10]   V. Pratap, A.K. Soni, S. Dayal, S.M. Abbas, A.M. Siddiqui, N.E. Prasad **465**, 540 (2018).

[11]   M.C. Dimri, S.C. Kashyap, D.C. Dube, IEEE Trans. Magn. **42**, 3635 (2006).

[12]   S. Kumar, R.S. Meena, R. Chatterjee J. Magn. Magn. Mater. **418**, 194 (2016).

[13]   R.S. Meena, S. Bhattacharya, R. Chatterjee, J. Magn. Magn. Mater. **322**, 2908 (2010).

[14]   R.S. Meena, S. Bhattacharya, R. Chatterjee, J. Magn. Magn. Mater. **322**, 1923 (2010).

[15]   K.P. Jeong, S.W. Yang, J.G. Kim, Arch. Metall. Mater. **63**, 3, 1447 (2018).

[16]   S. Yang, J.G. Kim, Arch. Metall. Mater. **62**, 2B, 1197 (2017).

[17]   S. Yang, K.P. Jeong, S.Y. Park, J.G. Kim, Arch. Metall. Mater. **62**, 2B, 1201 (2017).